How to cite: *Angew. Chem. Int. Ed.* **2020**, *59*, 18795 – 18803
International Edition: doi.org/10.1002/anie.202007144
German Edition: doi.org/10.1002/ange.202007144

C–C/H Activation

Regiodivergent C–H and Decarboxylative C–C Alkylation by Ruthenium Catalysis: *ortho* versus *meta* Position-Selectivity

*Korkit Korvorapun[+], Marc Moselage[+], Julia Struwe, Torben Rogge, Antonis M. Messinis, and Lutz Ackermann**

Abstract: *Ruthenium(II)biscarboxylate complexes enabled the selective alkylation of C–H and C–C bonds at the ortho- or meta-position. ortho-C–H Alkylations were achieved with 4-, 5- as well as 6-membered halocycloalkanes. Furthermore, the judicious choice of the directing group allowed for a full control of ortho-/meta-selectivities. Detailed mechanistic studies by experiment and computation were performed and provided strong support for an oxidative addition/reductive elimination process for ortho-alkylations, while a homolytic C–X cleavage was operative for the meta-selective transformations.*

Introduction

Methods for the direct modification of otherwise inert C–H bonds gained enormous attention throughout the last decade.[1] For the development of synthetically useful molecular transformations, the full control of positional selectivity is of prime importance for C–H functionalization reactions.[2] One important strategy for site-selective C–H activations is the use of chelation-assistance through the introduction of directing groups, thus allowing for proximity-induced *ortho*-C–H metalation.[3] During the past years, ruthenium catalysis was particularly recognized as an efficient tool for C–H functionalizations and a plethora of ruthenium-catalyzed C–H transformations was developed.[4] Especially, site-selective *ortho*-,[5] *meta*-[6] as well as *para*-alkylations[7] of arenes were devised by ruthenium catalysis, with major contributions by the groups of Frost,[8] and Ackermann,[9] among others.[10] Typically, secondary and tertiary alkyl halides result in C–H alkylations at the *meta*- or *para*-position with excellent levels of selectivity. In contrast, *ortho*-alkylated arenes were thus far predominantly obtained with primary alkyl halides (Scheme 1 a).

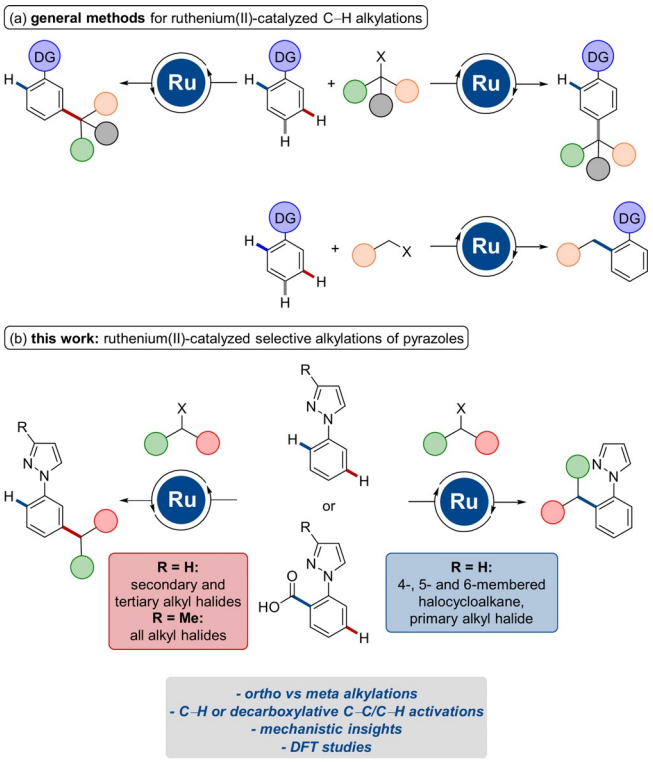

Scheme 1. Ruthenium-catalyzed site-selective alkylations.

Likewise, ruthenium catalysis proved to be powerful for C–C bond transformations, with notable progress by inter alia Dong and Hartwig.[11] Inspired by the versatility and robustness of the ruthenium catalyst, we became intrigued whether this C–C bond functionalization could be exploited for alkylation with unactivated alkyl halides.

Within our program on sustainable C–H activations,[12] we have now unraveled ruthenium-catalyzed *ortho*- or *meta*-alkylations through C–H or decarboxylative C–C/C–H activations (Scheme 1 b). Notable feature of our strategy include (i) versatile ruthenium-catalyzed *meta*- as well as *ortho*-alkylations with secondary alkyl bromides, (ii) functionalization of synthetically useful pyrazoles through C–H or decarboxylative C–C/C–H activations, (iii) detailed mechanistic insights by experiment, and (iv) DFT studies for ruthenium-catalyzed *ortho*-C–H alkylations.

[*] K. Korvorapun,[+] Dr. M. Moselage,[+] J. Struwe, Dr. T. Rogge, Dr. A. M. Messinis, Prof. Dr. L. Ackermann
Institut für Organische und Biomolekulare Chemie
Georg-August-Universität Göttingen
Tammannstrasse 2, 37077 Göttingen (Germany)
E-mail: Lutz.Ackermann@chemie.uni-goettingen.de
Homepage: http://www.ackermann.chemie.uni-goettingen.de/
[+] These authors contributed equally to this work.
Supporting information and the ORCID identification number(s) for the author(s) of this article can be found under https://doi.org/10.1002/anie.202007144.

Results and Discussion

In orienting experiments, we first examined the C–H alkylation of 2-phenylpyridine (**1**) with bromocyclohexane (**2a**), which provided the corresponding *meta*-alkylated product **4** in moderate yield (Scheme 2a). However, *ortho*-C–H alkylated product **6aa** was obtained when pyrazole **5a** was reacted with secondary alkyl bromide **2a** (Scheme 2b).

Intrigued by these unexpected results, we became interested in investigating the C–H alkylation of arylpyrazole **5a**. To this end, different reaction conditions were probed for the ruthenium-catalyzed C–H alkylation with bromocyclohexane (**2a**) (Table 1).[13] $PhCMe_3$[9f] proved to be the optimal solvent (entries 1–2). Furthermore, carboxylic acids[14] were found to be critical for achieving high conversions (entry 3). Previously, we and Larrosa had employed *p*-cymene-ligand-free ruthenium complexes for C–H activation.[5a,15] Cationic ruthenium(II) complexes could also here be employed as catalysts (entries 4–8). In addition, cyclohexyl chloride or iodide also afforded products **6aa** and **7aa** with positional selectivity, albeit in somewhat reduced yield (entries 9–10).

We next examined the effect of the halocycloalkane **2** ring size on the site-selectivity of the C–H alkylation reaction (Scheme 3). The reaction of unsubstituted phenylpyrazole **5a** with bromocyclobutane (**2b**) and bromocyclohexane (**2a**) afforded the *ortho*-alkylated products **6aa** and **6ab** as the major product, whereas bromocycloheptane (**2d**) and bromocyclooctane (**2e**) preferentially furnished the *meta*-alkylated products **7** (Scheme 3a). In contrast, bromocyclopentane (**2c**) yielded a mixture of the *ortho*- and *meta*-alkylated products **6ac** and **7ac**. Then, we probed the alkylation of

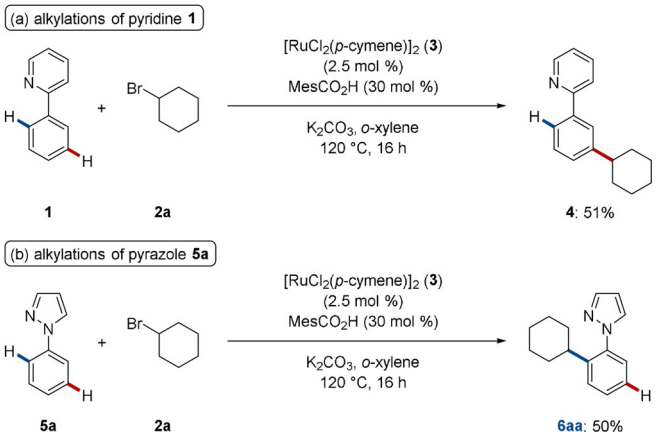

Scheme 2. Site-selective C–H alkylations.

Table 1: Ruthenium-catalyzed C–H alkylation of pyrazole **5a**

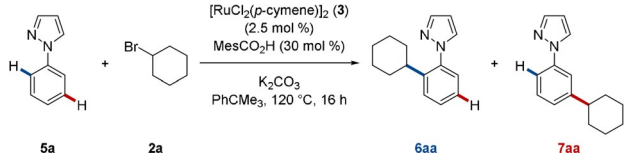

Entry	Deviation from the standard conditions	**6aa** [%]	**7aa** [%]
1	none	60	12
2	*o*-xylene instead of $PhCMe_3$	50	–
3	without $MesCO_2H$	28	–
4	$[Ru(NCt\text{-}Bu)_6][BF_4]_2$ instead of **3**	60	8
5	$[Ru(NCt\text{-}Bu)_6][PF_6]_2$ instead of **3**	62	10
6	$[Ru(NCt\text{-}Bu)_6][SbF_6]_2$ instead of **3**	63	9
7	$[Ru(NCMe)_6][PF_6]_2$ instead of **3**	65	12
8	$[Ru(NCMe)_6][PF_6]_2$ instead of **3** and without $MesCO_2H$	–	–
9	Cy-Cl instead of **2a**	38	5
10	Cy-I instead of **2a**	53	7

[a] Reaction conditions: **5a** (0.5 mmol), **2a** (1.5 mmol), [Ru] (5.0 mol%), $MesCO_2H$ (30 mol%), K_2CO_3 (1.0 mmol), $PhCMe_3$ (1.0 mL), 120°C, 16 h, yields of isolated products.

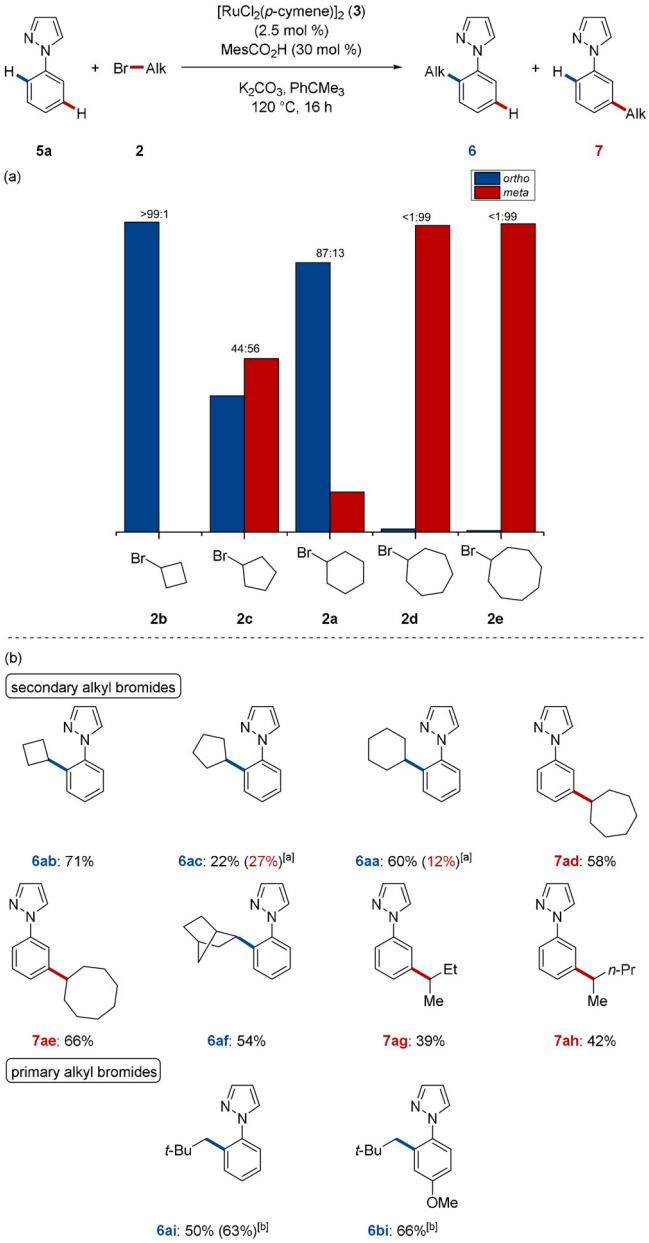

Scheme 3. (a) Site-selectivity of ruthenium-catalyzed C–H alkylations of pyrazole **5a** with various bromocycloalkanes **2**, (b) scope for C–H alkylation of pyrazoles **5**. [a] The yield of *meta*-alkylated product **7** is given in parentheses. [b] *o*-Xylene was used as solvent.

arylpyrazoles **5** with primary as well as secondary alkyl bromides **2** (Scheme 3b). The alkylation reaction of arylpyrazoles **5** with *exo*-2-bromonorbornane (**2f**) or neopentyl bromide (**2i**) afforded the *ortho*-alkylated products **6af**, **6ai**, and **6bi** exclusively. Acyclic secondary alkyl bromides **2g** and **2h** were smoothly converted into *meta*-alkylated products **7ag** and **7ah** with excellent levels of positional selectivity.

Next, the electronic effect on the site-selectivity was studied with differently substituted arylpyrazoles **5** with cyclohexyl bromide (**2a**) (Scheme 4). Electron-donating groups at the *para*-position led to a mixture of *ortho*- and *meta*-alkylated products **6** and **7**, whereas electron-withdrawing groups exclusively afforded the *ortho*-alkylated products (**6da**–**6fa**). The connectivity of product **6fa** was unambiguously assigned by X-ray diffraction analysis.[16]

In contrast to arylpyrazoles **5a**–**5f**, the direct alkylation of 3,5-dimethyl-1-phenyl-1*H*-pyrazole (**5g**) with cyclic and acyclic secondary alkyl bromides **2** exclusively provided the *meta*-alkylated products **7** (Scheme 5). In addition, the alkylation with neopentyl bromide (**2i**) selectively furnished the *meta*-alkylated adduct **7gi**, albeit in lower yield.

To understand the nature of the reaction mechanism, the alkylation reaction was conducted in the presence of typical radical scavengers (Scheme 6a). While 2,2,6,6-tetramethylpiperidin-1-oxyl (TEMPO) fully inhibited the catalytic reaction, the use of 1,1-diphenylethylene significantly reduced the yield of the corresponding product **6aa**. The isolation of adduct **8** was supportive of a homolytic C–X bond cleavage. The reaction mechanism was further elucidated by the use of diastereomerically pure electrophiles **2j** and **2k** (Scheme 6b). The reaction with *endo*-2-bromobornane (*endo*-**2j**) provided *ortho*-alkylated product *endo*-**6fj** as well as a diastereomeric mixture of *meta*-alkylated products **7fj**. Similarly, the stereochemistry of *tert*-butylcyclohexyl bromide *cis*-**2k** and *trans*-**2k**[9f,17] translated directly into the corresponding *ortho*-alkylated products *cis*-**6fk** and *trans*-**6fk**, respectively. These findings thus provide strong support for a concerted oxidative addition/reductive elimination mechanism to be operative for the *ortho*-alkylation. In contrast, the *meta*-functionalized product **7fk** was obtained as *cis*- and *trans*-isomers from the reaction with the single isomer *cis*-**2k**, which is indicative of the formation of an alkyl radical via a single-electron transfer (SET) process. The stereochemistry and site-selectivity of products **6** and **7** were confirmed by X-ray analysis.[16]

Furthermore, we prepared the well-defined cationic cyclometalated ruthenium complexes **Ru I** and **Ru II**,[13] which showed high catalytic activity in the presence of $MesCO_2H$ (Scheme 7a). In contrast to the standard condition, the reaction of phenylpyrazole **5g** in the absence of an acid additive resulted in a mixture of *ortho*- and *meta*-alkylated products **6ga** and **7ga**. In addition, a substantial amount of decoordinated *p*-cymene was observed in the initial period of the alkylation reaction (Scheme 7b).

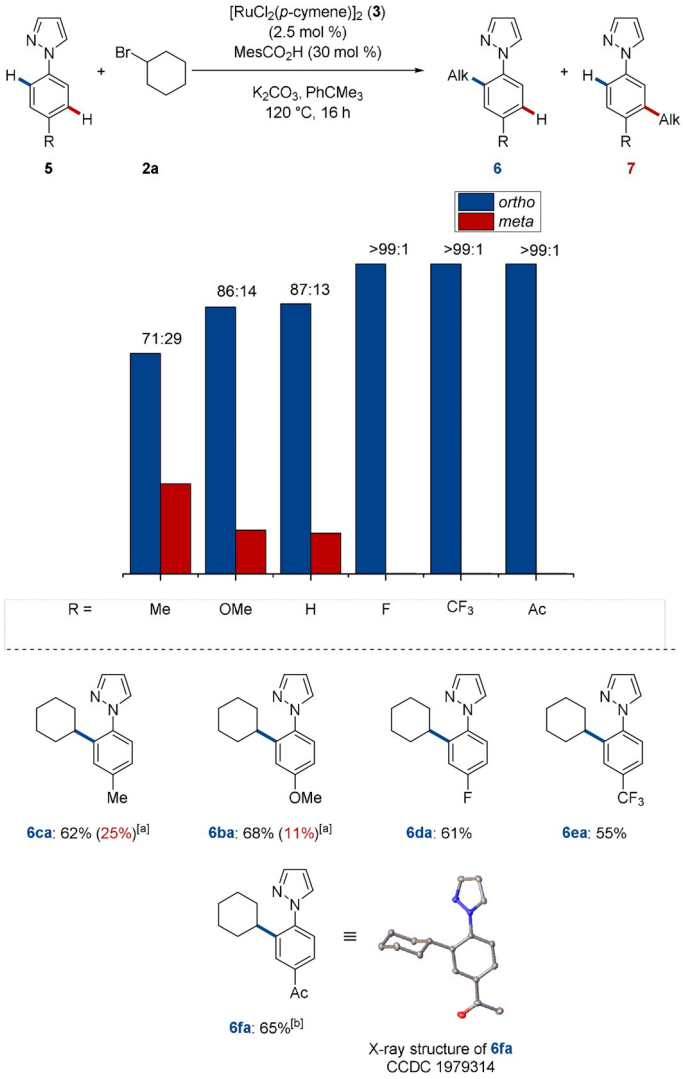

Scheme 4. Electronic effect on the site-selectivity of ruthenium-catalyzed C–H alkylations of arylpyrazoles **5** with bromocyclohexane (**2a**). [a] The yield of *meta*-alkylated product **7** is given in parentheses. [b] Dialkylated product was obtained in 29% yield.

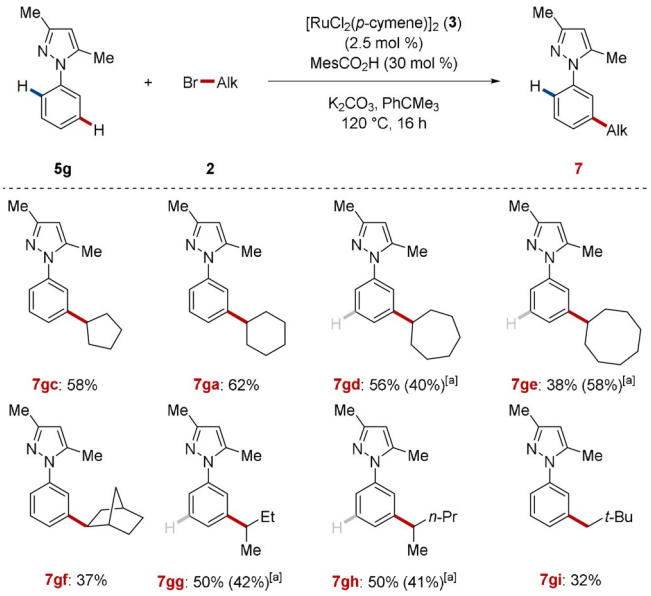

Scheme 5. Ruthenium-catalyzed C–H alkylation of phenylpyrazole **5g**. [a] The yield of di-*meta*-alkylated product is given in parentheses.

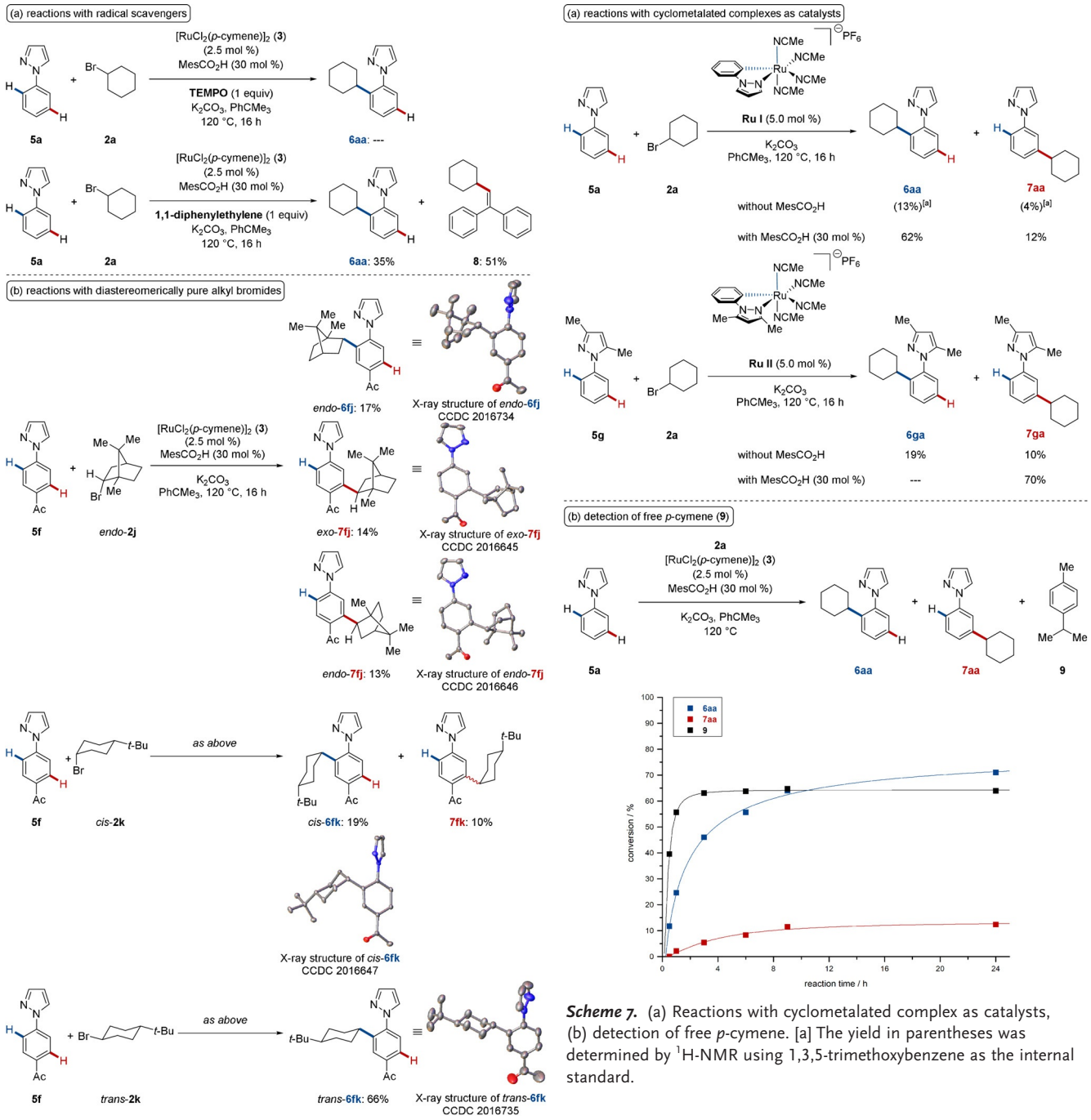

Scheme 7. (a) Reactions with cyclometalated complex as catalysts, (b) detection of free *p*-cymene. [a] The yield in parentheses was determined by ^{1}H-NMR using 1,3,5-trimethoxybenzene as the internal standard.

Scheme 6. Key mechanistic studies: (a) reaction in the presence of radical scavengers, (b) C–H alkylations with diastereomerically pure alkyl bromides **2**.

Mechanistic studies by means of density functional theory (DFT) calculations were next conducted at the PW6B95-D3(BJ)/def2-TZVP + COSMO(*o*-xylene)//TPSS-D3(BJ)/def2-TZVP level of theory.[18] These findings reveal a facile oxidative addition of cyclohexyl bromide/reductive elimination process to occur on biscyclometalated ruthenium(II) intermediates with an energy barrier of only 17.6 kcal mol^{-1} (Figure 1). Calculations with various substituted arylpyrazoles indicated a rather minor influence of the substrate's electronic properties on the energy barriers for the oxidative addition/reductive elimination elementary steps.

A distortion energy analysis of **TS2** with different directing groups revealed a substantially increased distortion energy, when the 3,5-dimethylpyrazole was employed (Figure 2).[13]

Furthermore, the ruthenium(II)carboxylate catalysis was also found to facilitate decarboxylative alkylation reactions. Here various reaction conditions for the envisioned decarboxylative alkylation reaction of acid **10a** with bromocycloheptane (**2d**) were tested first (Table 2).[13] Carboxylate assistance significantly improved the catalytic efficacy, with $MesCO_2H$ being the optimal acid additive (entries 1–4).[14b] The reaction without an acid additive gave a reduced yield

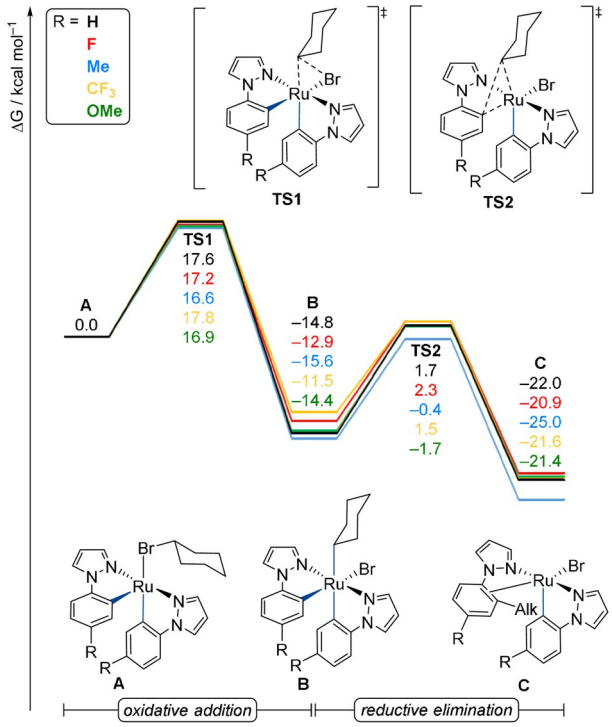

Figure 1. Relative Gibbs free energy profile for the oxidative addition/reductive elimination elementary step at the PW6B95-D3(BJ)/def2-TZVP + COSMO(*o*-xylene)//TPSS-D3(BJ)/def2-TZVP level of theory.

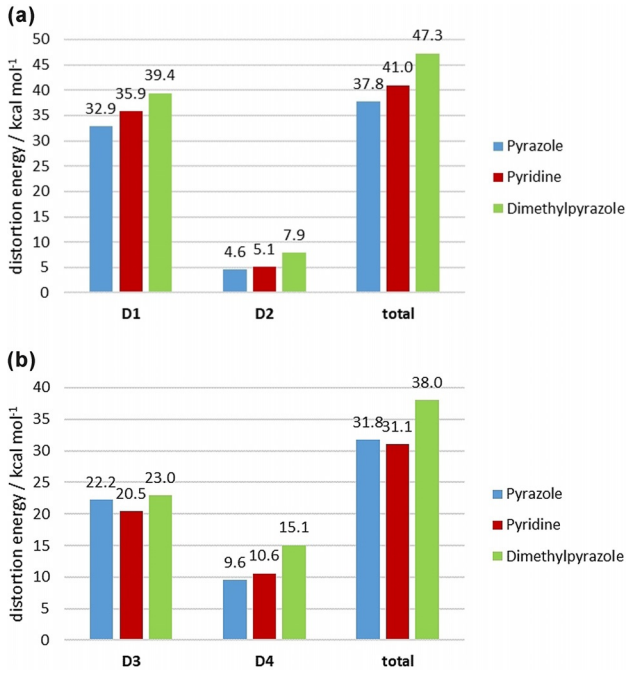

Figure 2. Distortion energy (a) for reductive elimination with different heterocycles, (b) for radical addition with *N*-heterocycles.

(entry 2), presumably because the substrate **10a** can itself act as carboxylate ligand. Control experiments verified the essential role of the ruthenium catalyst (entry 5). Furthermore, the well-defined complex $[Ru(O_2CMes)_2(p\text{-cymene})]$[19] turned out to be a competent catalyst (entry 6). To our delight, the reaction also proceeded under arene-ligand-free conditions using ruthenium-nitrile complexes (entries 7–8). Other ruthenium sources such as $Ru_3(CO)_{12}$ and $RuCl_3 \cdot (H_2O)_n$ failed to facilitate any conversion (entries 9–10). Moreover, no product formation was observed when the reaction was attempted with palladium, rhodium, cobalt, or nickel complexes.[13]

Table 2: Optimization of ruthenium-catalyzed decarboxylative C–C alkylation of **10a**

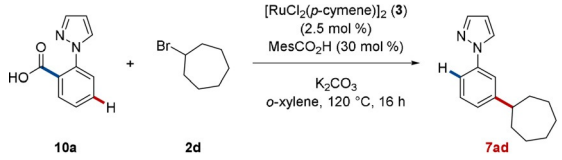

Entry	Deviation from the standard conditions	Yield (%)
1	none	73
2	without $MesCO_2H$	39
3	1-AdCO_2H instead of $MesCO_2H$	49
4	PivOH instead of $MesCO_2H$	56
5	without **3**	–
6	$[Ru(O_2CMes)_2(p\text{-cymene})]$ instead of **3** and without $MesCO_2H$	70
7	$[Ru(NCt\text{-}Bu)_6][BF_4]_2$ instead of **3**	60
8	$[Ru(NCt\text{-}Bu)_6][SbF_6]_2$ instead of **3**	49
9	$RuCl_3 \cdot (H_2O)_n$ instead of **3**	–
10	$Ru_3(CO)_{12}$ instead of **3**	–
11	$Pd(OAc)_2$, $[Cp^*RhCl_2]_2$, $[Cp^*Co(CO)I_2]$ or $[Ni(cod)_2]$ as catalysts	–

[a] Reaction conditions: **10a** (0.5 mmol), **2d** (1.5 mmol), [Ru] (5.0 mol%), additive (30 mol%), K_2CO_3 (1.0 mmol), *o*-xylene (1.0 mL), 120 °C, 16 h, yields of isolated products.

Having identified the optimal reaction conditions, we tested the versatility towards different alkyl bromides **2** (Scheme 8). With primary alkyl bromides **2i–2m**, the C–H alkylation took place at the *ortho*-position with excellent levels of regioselectivity. It is noteworthy that the reaction of acid **10i** and neopentyl bromide (**2i**) afforded 40% of the desired product **6ii** and 37% of the *ortho*-xylylated product **6ii′** as a side-product,[16] which presumably forms via H-atom abstraction from the *o*-xylene solvent followed by benzylation. Similar to the C–H alkylation reaction (vide supra), the decarboxylative alkylation of bromocyclohexane (**2a**) and *exo*-2-bromonorbornane (**2f**) furnished the *ortho*-alkylated products **6aa**, **6af**, and **6if** with excellent levels of site-selectivity. In contrast, reactions with a broad range of acyclic alkyl bromides as well as cyclic alkyl bromides resulted in a preferred *meta*-alkylation.[16] Inspired by a recent *meta*-selective alkylation with α-bromoesters from our group,[9c] we probed whether this reaction can be combined with a C–C cleavage step. Indeed, slightly modified reaction conditions allowed for the formation of the products **7ap–7jp** via C–C/C–H activation in high yields. Moreover, tertiary alkyl bromides reacted in the decarboxylative alkylation regime solely with *meta*-selectivity.

Finally, ozonolysis[20] of the alkylated arenes **6** or **7** provided access to synthetically useful *meta*-alkylated aceta-

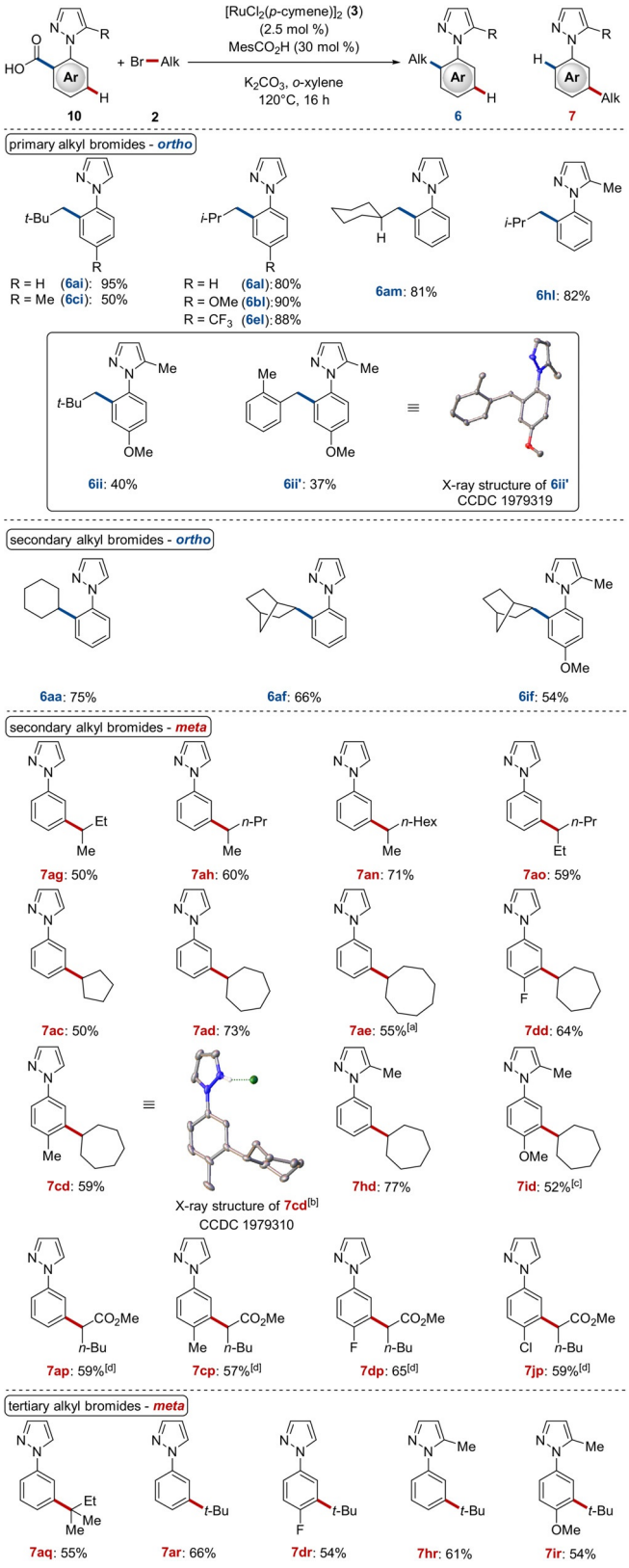

Scheme 8. Ruthenium-catalyzed decarboxylative C–C alkylation. [a] $[RuCl_2(p\text{-cymene})]_2$ (5.0 mol%). [b] HCl adduct. [c] *n*-Octane instead of *o*-xylene as solvent. [d] PPh_3 (5.0 mol%), $PhCMe_3$ instead of *o*-xylene.

nilides **11** in remarkably good yields, highlighting the versatility of the ruthenium-catalyzed direct C–H alkylation (Scheme 9).[16]

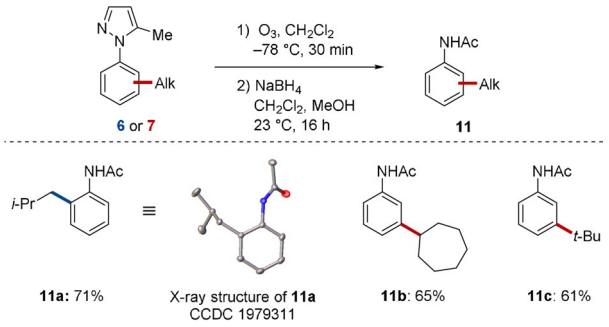

Scheme 9. Product diversification by ozonolysis.

Given the broad applicability of this decarboxylative alkylation reaction, we became interested in unraveling its mode of action. To this end, detailed mechanistic studies were performed (Scheme 10). Reactions with radical scavengers led to a complete or partial inhibition of the catalytic activity (Scheme 10a). In the presence of TEMPO, the alkyl-TEMPO adduct **12** could be detected and isolated, which is in line with a radical C–X bond cleavage. Reactions in the presence of deuterated co-solvents clearly indicated the organometallic character of the C–C cleavage (Scheme 10b). In the absence of an alkyl bromide, almost complete decarboxylation took place and significant deuterium incorporation was observed at the *ortho*-position and partly at the C3 and C5 position of the pyrazole, presumably due to electrophilic activation. In the presence of alkyl bromide **2d**, a deuterium incorporation of 46% and 47% was observed at the *ortho*-position of alkylated product $[D]_n$-**7ad**. A considerable decoordination of *p*-cymene was detected during the initial period of the decarboxylative alkylation (Scheme 10c).

On the basis of our findings, a plausible catalytic cycle for the *ortho*-selective alkylation commences by a carboxylate-assisted C–H ruthenation and dissociation of *p*-cymene, thereby forming the cyclometalated complex **14** (Scheme 11, left). A second molecule of phenylpyrazole **5** coordinates to ruthenium complex **14** and undergoes C–H activation to form biscyclometalated complex **15**. The oxidative addition of alkyl bromide **2** to complex **15** generates the stable ruthenium(IV) intermediate **16**/**B** (Figure 1). Finally, reductive elimination and ligand exchange deliver the *ortho*-alkylated product **6** and ruthenacycle **14**. In contrast, *meta*-C–H alkylation occurs through a SET process from ruthenium(II) complex **14** to alkyl bromide **2**, forming ruthenium(III) intermediate **18** and a stabilized alkyl radical **19** (Scheme 11, right). Subsequently, **19** preferentially attacks the position *para* to ruthenium, thus leading to the formation of triplet ruthenium intermediate **20**.[9a,c] Ligand-to-metal electron transfer and rearomatization furnishes ruthenacycle **21**, which undergoes protodemetalation and C–H activation to furnish the desired *meta*-alkylated product **7** and regenerates the active ruthenium species **14**.

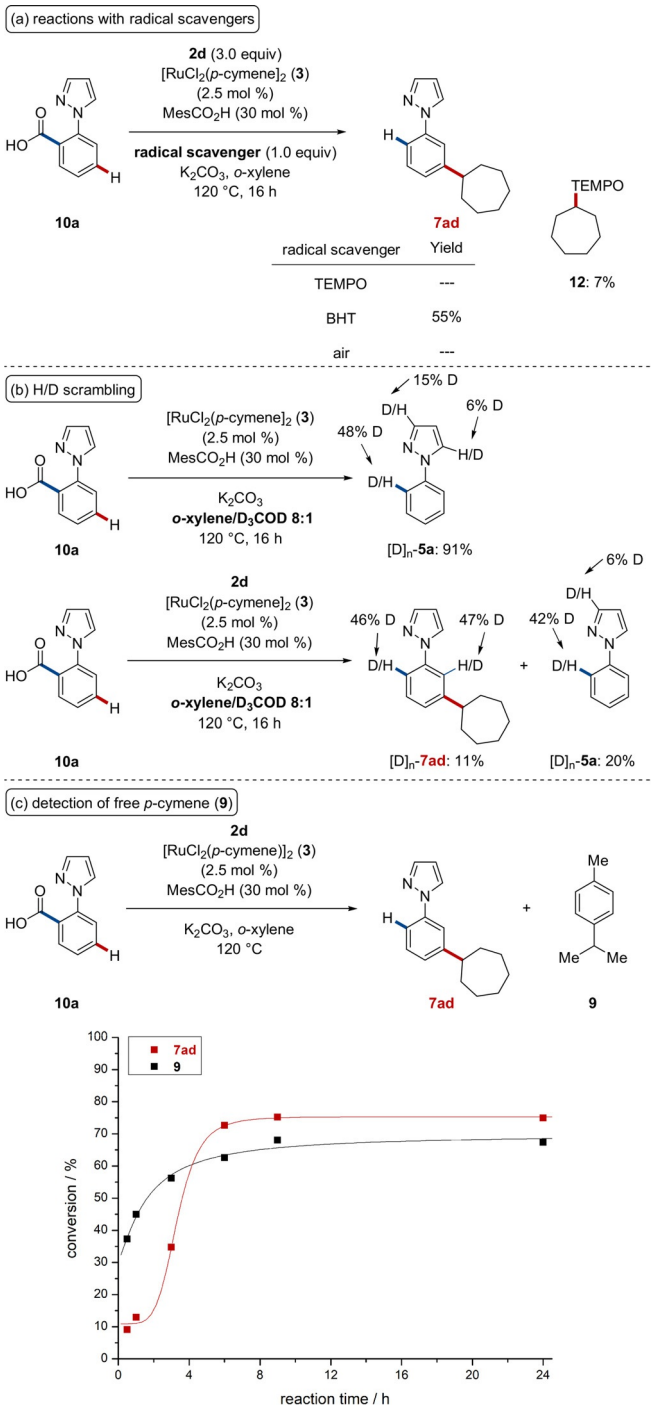

Scheme 10. Key mechanistic findings: (a) reaction in the presence of radical scavengers, (b) H/D scrambling experiments, (c) detection of free *p*-cymene.

Conclusion

In summary, we have reported on a ruthenium-catalyzed C–H and C–C activation allowing for *ortho*- and *meta*-alkylations of synthetically useful pyrazoles. The steric properties of the employed alkyl bromides and pyrazoles had a significant influence on the position-selectivity of the alkylation reaction. Mechanistic studies were suggestive of two distinct mechanisms, an oxidative addition/reductive elimination event for the *ortho*-C–H alkylation, while a SET pathway is proposed for *meta*-functionalization. Moreover, an arene-ligand-free ruthenacycles was identified as the key intermediate in this transformation. Furthermore, computational studies and experiments with diastereomerically pure alkyl bromides unraveled an energetically favorable novel mechanism for *ortho*-C–H secondary alkylations.

Acknowledgements

Generous support by the DAAD (fellowship to K.K.) and the DFG (SPP1807 and Gottfried-Wilhelm-Leibniz prize) is gratefully acknowledged. We thank Dr. Christopher Golz (University Göttingen) for the X-ray diffraction analysis. Open access funding enabled and organized by Projekt DEAL.

Conflict of interest

The authors declare no conflict of interest.

Keywords: alkylation · C–C activation · C–H activation · decarboxylation · ruthenium

[1] For selected reviews, see: a) S. Rej, Y. Ano, N. Chatani, *Chem. Rev.* **2020**, *120*, 1788–1887; b) P. Gandeepan, T. Müller, D. Zell, G. Cera, S. Warratz, L. Ackermann, *Chem. Rev.* **2019**, *119*, 2192–2452; c) C.-S. Wang, P. H. Dixneuf, J.-F. Soulé, *Chem. Rev.* **2018**, *118*, 7532–7585; d) C. G. Newton, S.-G. Wang, C. C. Oliveira, N. Cramer, *Chem. Rev.* **2017**, *117*, 8908–8976; e) Y. Park, Y. Kim, S. Chang, *Chem. Rev.* **2017**, *117*, 9247–9301; f) T. Gensch, M. N. Hopkinson, F. Glorius, J. Wencel-Delord, *Chem. Soc. Rev.* **2016**, *45*, 2900–2936; g) V. Ritleng, C. Sirlin, M. Pfeffer, *Chem. Rev.* **2002**, *102*, 1731–1770.

[2] For selected reviews, see: a) S. M. Khake, N. Chatani, *Trends Chem.* **2019**, *1*, 524–539; b) Y. Kommagalla, N. Chatani, *Coord. Chem. Rev.* **2017**, *350*, 117–135; c) D. A. Colby, A. S. Tsai, R. G. Bergman, J. A. Ellman, *Acc. Chem. Res.* **2012**, *45*, 814–825; d) S. R. Neufeldt, M. S. Sanford, *Acc. Chem. Res.* **2012**, *45*, 936–946; e) D. A. Colby, R. G. Bergman, J. A. Ellman, *Chem. Rev.* **2010**, *110*, 624–655; f) T. W. Lyons, M. S. Sanford, *Chem. Rev.* **2010**, *110*, 1147–1169; g) L. Ackermann, R. Vicente, A. R. Kapdi, *Angew. Chem. Int. Ed.* **2009**, *48*, 9792–9826; *Angew. Chem.* **2009**, *121*, 9976–10011.

[3] For selected reviews on chelation-assisted C–H functionalization, see: a) C. Sambiagio, D. Schönbauer, R. Blieck, T. Dao-Huy, G. Pototschnig, P. Schaaf, T. Wiesinger, M. F. Zia, J. Wencel-Delord, T. Besset, B. U. W. Maes, M. Schnürch, *Chem. Soc. Rev.* **2018**, *47*, 6603–6743; b) Z. Chen, B. Wang, J. Zhang, W. Yu, Z. Liu, Y. Zhang, *Org. Chem. Front.* **2015**, *2*, 1107–1295; c) Z. Huang, H. N. Lim, F. Mo, M. C. Young, G. Dong, *Chem. Soc. Rev.* **2015**, *44*, 7764–7786; d) F. Zhang, D. R. Spring, *Chem. Soc. Rev.* **2014**, *43*, 6906–6919.

[4] For selected reviews on ruthenium-catalyzed C–H functionalization, see: a) C. Shan, L. Zhu, L.-B. Qu, R. Bai, Y. Lan, *Chem. Soc. Rev.* **2018**, *47*, 7552–7576; b) P. Nareddy, F. Jordan, M. Szostak, *ACS Catal.* **2017**, *7*, 5721–5745; c) L. Ackermann, *Acc. Chem. Res.* **2014**, *47*, 281–295; d) S. De Sarkar, W. Liu, S. I. Kozhushkov, L. Ackermann, *Adv. Synth. Catal.* **2014**, *356*, 1461–1479; e) P. B. Arockiam, C. Bruneau, P. H. Dixneuf, *Chem. Rev.*

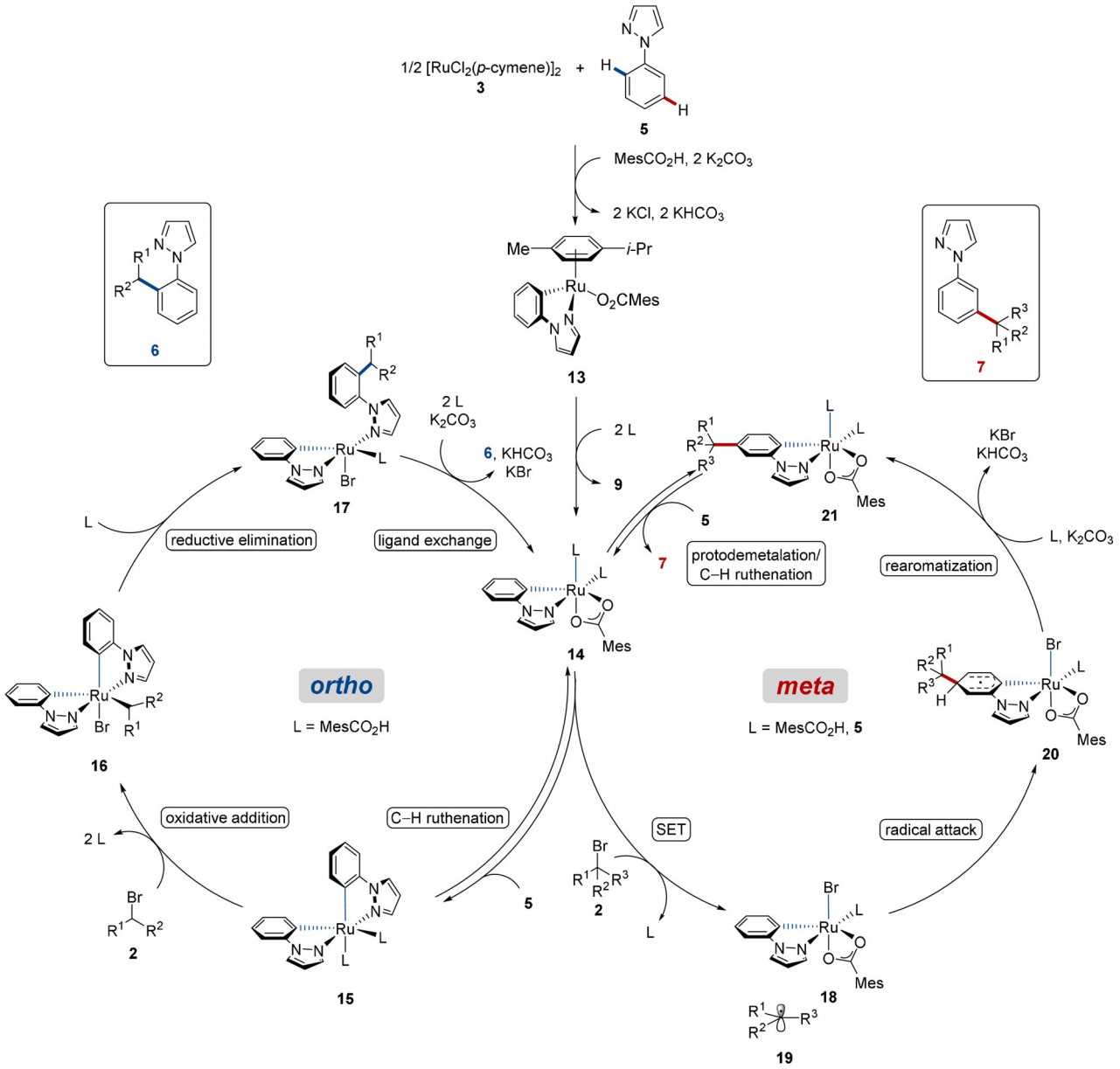

Scheme 11. Proposed catalytic cycle for ruthenium-catalyzed *ortho*- or *meta*-alkylation.

2012, *112*, 5879 – 5918; f) F. Kakiuchi, N. Chatani, *Adv. Synth. Catal.* **2003**, *345*, 1077 – 1101.

[5] a) G.-W. Wang, M. Wheatley, M. Simonetti, D. M. Cannas, I. Larrosa, *Chem* **2020**, *6*, 1459 – 1468; b) L. Ackermann, N. Hofmann, R. Vicente, *Org. Lett.* **2011**, *13*, 1875 – 1877; c) L. Ackermann, P. Novák, R. Vicente, N. Hofmann, *Angew. Chem. Int. Ed.* **2009**, *48*, 6045 – 6048; *Angew. Chem.* **2009**, *121*, 6161 – 6164; d) L. Ackermann, P. Novák, *Org. Lett.* **2009**, *11*, 4966 – 4969.

[6] For selected reviews on ruthenium-catalyzed *meta*-C–H functionalization, see: a) M. T. Mihai, G. R. Genov, R. J. Phipps, *Chem. Soc. Rev.* **2018**, *47*, 149 – 171; b) J. A. Leitch, C. G. Frost, *Chem. Soc. Rev.* **2017**, *46*, 7145 – 7153; c) J. Li, S. De Sarkar, L. Ackermann, *Top. Organomet. Chem.* **2016**, *55*, 217 – 257.

[7] a) C. Yuan, L. Zhu, C. Chen, X. Chen, Y. Yang, Y. Lan, Y. Zhao, *Nat. Commun.* **2018**, *9*, 1189; b) C. Yuan, L. Zhu, R. Zeng, Y. Lan, Y. Zhao, *Angew. Chem. Int. Ed.* **2018**, *57*, 1277 – 1281; *Angew. Chem.* **2018**, *130*, 1291 – 1295; c) X.-G. Wang, Y. Li, L.-L. Zhang, B.-S. Zhang, Q. Wang, J.-W. Ma, Y.-M. Liang, *Chem. Commun.* **2018**, *54*, 9541 – 9544; d) J. A. Leitch, C. L. McMullin, A. J. Paterson, M. F. Mahon, Y. Bhonoah, C. G. Frost, *Angew. Chem. Int. Ed.* **2017**, *56*, 15131 – 15135; *Angew. Chem.* **2017**, *129*, 15327 – 15331.

[8] a) A. J. Paterson, C. J. Heron, C. L. McMullin, M. F. Mahon, N. J. Press, C. G. Frost, *Org. Biomol. Chem.* **2017**, *15*, 5993 – 6000; b) A. J. Paterson, S. St John-Campbell, M. F. Mahon, N. J. Press, C. G. Frost, *Chem. Commun.* **2015**, *51*, 12807 – 12810.

[9] a) K. Korvorapun, R. Kuniyil, L. Ackermann, *ACS Catal.* **2020**, *10*, 435 – 440; b) P. Gandeepan, J. Koeller, K. Korvorapun, J. Mohr, L. Ackermann, *Angew. Chem. Int. Ed.* **2019**, *58*, 9820 – 9825; *Angew. Chem.* **2019**, *131*, 9925 – 9930; c) K. Korvorapun, N. Kaplaneris, T. Rogge, S. Warratz, A. C. Stückl, L. Ackermann, *ACS Catal.* **2018**, *8*, 886 – 892; d) F. Fumagalli, S. Warratz, S.-K. Zhang, T. Rogge, C. Zhu, A. C. Stückl, L. Ackermann, *Chem. Eur. J.* **2018**, *24*, 3984 – 3988; e) Z. Ruan, S.-K. Zhang, C. Zhu, P. N. Ruth, D. Stalke, L. Ackermann, *Angew. Chem. Int. Ed.*

2017, *56*, 2045 – 2049; *Angew. Chem.* **2017**, *129*, 2077 – 2081; f) J. Li, K. Korvorapun, S. De Sarkar, T. Rogge, D. J. Burns, S. Warratz, L. Ackermann, *Nat. Commun.* **2017**, *8*, 15430; g) J. Li, S. Warratz, D. Zell, S. De Sarkar, E. E. Ishikawa, L. Ackermann, *J. Am. Chem. Soc.* **2015**, *137*, 13894 – 13901; h) N. Hofmann, L. Ackermann, *J. Am. Chem. Soc.* **2013**, *135*, 5877 – 5884.

[10] a) G. Li, C. Jia, X. Cai, L. Zhong, L. Zou, X. Cui, *Chem. Commun.* **2020**, *56*, 293 – 296; b) C. Jia, S. Wang, X. Lv, G. Li, L. Zhong, L. Zou, X. Cui, *Eur. J. Org. Chem.* **2020**, 1992 – 1995; c) A. Sagadevan, M. F. Greaney, *Angew. Chem. Int. Ed.* **2019**, *58*, 9826 – 9830; *Angew. Chem.* **2019**, *131*, 9931 – 9935; d) B. Li, S.-L. Fang, D.-Y. Huang, B.-F. Shi, *Org. Lett.* **2017**, *19*, 3950 – 3953; e) G. Li, P. Gao, X. Lv, C. Qu, Q. Yan, Y. Wang, S. Yang, J. Wang, *Org. Lett.* **2017**, *19*, 2682 – 2685; f) G. Li, D. Li, J. Zhang, D.-Q. Shi, Y. Zhao, *ACS Catal.* **2017**, *7*, 4138 – 4143; g) G. Li, X. Ma, C. Jia, Q. Han, Y. Wang, J. Wang, L. Yu, S. Yang, *Chem. Commun.* **2017**, *53*, 1261 – 1264; h) Z.-Y. Li, L. Li, Q.-L. Li, K. Jing, H. Xu, G.-W. Wang, *Chem. Eur. J.* **2017**, *23*, 3285 – 3290.

[11] For selected examples of transition metal-catalyzed C–C activations, see: a) S.-H. Hou, A. Y. Prichina, M. Zhang, G. Dong, *Angew. Chem. Int. Ed.* **2020**, *59*, 7848 – 7856; *Angew. Chem.* **2020**, *132*, 7922 – 7930; b) Z. Hu, X.-Q. Hu, G. Zhang, L. J. Gooßen, *Org. Lett.* **2019**, *21*, 6770 – 6773; c) J. Zhu, P.-h. Chen, G. Lu, P. Liu, G. Dong, *J. Am. Chem. Soc.* **2019**, *141*, 18630 – 18640; d) J. Zhu, J. Wang, G. Dong, *Nat. Chem.* **2019**, *11*, 45 – 51; e) L. Deng, Y. Fu, S. Y. Lee, C. Wang, P. Liu, G. Dong, *J. Am. Chem. Soc.* **2019**, *141*, 16260 – 16265; f) T. Sun, Y. Zhang, B. Qiu, Y. Wang, Y. Qin, G. Dong, T. Xu, *Angew. Chem. Int. Ed.* **2018**, *57*, 2859 – 2863; *Angew. Chem.* **2018**, *130*, 2909 – 2913; g) Z. Zhu, X. Li, S. Chen, P.-h. Chen, B. A. Billett, Z. Huang, G. Dong, *ACS Catal.* **2018**, *8*, 845 – 849; h) H. Wang, I. Choi, T. Rogge, N. Kaplaneris, L. Ackermann, *Nat. Catal.* **2018**, *1*, 993 – 1001; i) M. Moselage, J. Li, F. Kramm, L. Ackermann, *Angew. Chem. Int. Ed.* **2017**, *56*, 5341 – 5344; *Angew. Chem.* **2017**, *129*, 5425 – 5428; j) N. Y. P. Kumar, A. Bechtoldt, K. Raghuvanshi, L. Ackermann, *Angew. Chem. Int. Ed.* **2016**, *55*, 6929 – 6932; *Angew. Chem.* **2016**, *128*, 7043 – 7046; k) J. Zhang, R. Shrestha, J. F. Hartwig, P. Zhao, *Nat. Chem.* **2016**, *8*, 1144 – 1151; l) L. Huang, A. Biafora, G. Zhang, V. Bragoni, L. J. Gooßen, *Angew. Chem. Int. Ed.* **2016**, *55*, 6933 – 6937; *Angew. Chem.* **2016**, *128*, 7047 – 7051; m) E. Ozkal, B. Cacherat, B. Morandi, *ACS Catal.* **2015**, *5*, 6458 – 6462; n) N. Ishida, W. Ikemoto, M. Murakami, *J. Am. Chem. Soc.* **2014**, *136*, 5912 – 5915; o) L. Souillart, N. Cramer, *Angew. Chem. Int. Ed.* **2014**, *53*, 9640 – 9644; *Angew. Chem.* **2014**, *126*, 9794 – 9798; p) T. Seiser, N. Cramer, *J. Am. Chem. Soc.* **2010**, *132*, 5340 – 5341; q) T. Seiser, O. A. Roth, N. Cramer, *Angew. Chem. Int. Ed.* **2009**, *48*, 6320 – 6323; *Angew. Chem.* **2009**, *121*, 6438 – 6441; r) N. Chatani, Y. Ie, F. Kakiuchi, S. Murai, *J. Am. Chem. Soc.* **1999**, *121*, 8645 – 8646.

[12] L. Ackermann, *Acc. Chem. Res.* **2020**, *53*, 84 – 104.

[13] For detailed information, see the Supporting Information.

[14] a) D. L. Davies, S. A. Macgregor, C. L. McMullin, *Chem. Rev.* **2017**, *117*, 8649 – 8709; b) L. Ackermann, *Chem. Rev.* **2011**, *111*, 1315 – 1345.

[15] a) T. Rogge, L. Ackermann, *Angew. Chem. Int. Ed.* **2019**, *58*, 15640 – 15645; *Angew. Chem.* **2019**, *131*, 15787 – 15792; b) M. Simonetti, D. M. Cannas, X. Just-Baringo, I. J. Vitorica-Yrezabal, I. Larrosa, *Nat. Chem.* **2018**, *10*, 724 – 731; c) M. Simonetti, D. M. Cannas, A. Panigrahi, S. Kujawa, M. Kryjewski, P. Xie, I. Larrosa, *Chem. Eur. J.* **2017**, *23*, 549 – 553; d) L. Ackermann, A. Althammer, R. Born, *Tetrahedron* **2008**, *64*, 6115 – 6124; e) L. Ackermann, A. Althammer, R. Born, *Synlett* **2007**, 2833 – 2836; f) L. Ackermann, R. Born, P. Álvarez-Bercedo, *Angew. Chem. Int. Ed.* **2007**, *46*, 6364 – 6367; *Angew. Chem.* **2007**, *119*, 6482 – 6485.

[16] Deposition numbers 1979314 (**6fa**), 2016734 (*endo*-**6fj**), 2016645 (*exo*-**7fj**), 2016646 (*endo*-**7fj**), 2016647 (*cis*-**6fk**), 2016735 (*trans*-**6fk**), 1979319 (**6ii′**), 1979310 (**7cd**), and 1979311 (**11a**) contain the supplementary crystallographic data for this paper. These data are provided free of charge by the joint Cambridge Crystallographic Data Centre and Fachinformationszentrum Karlsruhe Access Structures service.

[17] G. Cera, T. Haven, L. Ackermann, *Angew. Chem. Int. Ed.* **2016**, *55*, 1484 – 1488; *Angew. Chem.* **2016**, *128*, 1506 – 1510.

[18] a) S. Grimme, S. Ehrlich, L. Goerigk, *J. Comput. Chem.* **2011**, *32*, 1456 – 1465; b) S. Grimme, J. Antony, S. Ehrlich, H. Krieg, *J. Chem. Phys.* **2010**, *132*, 154104; c) S. Sinnecker, A. Rajendran, A. Klamt, M. Diedenhofen, F. Neese, *J. Phys. Chem. A* **2006**, *110*, 2235 – 2245; d) Y. Zhao, D. G. Truhlar, *J. Phys. Chem. A* **2005**, *109*, 5656 – 5667; e) F. Weigend, R. Ahlrichs, *Phys. Chem. Chem. Phys.* **2005**, *7*, 3297 – 3305; f) J. Tao, J. P. Perdew, V. N. Staroverov, G. E. Scuseria, *Phys. Rev. Lett.* **2003**, *91*, 146401; g) A. Klamt, V. Jonas, T. Bürger, J. C. W. Lohrenz, *J. Phys. Chem. A* **1998**, *102*, 5074 – 5085; h) A. Klamt, *J. Phys. Chem.* **1995**, *99*, 2224 – 2235.

[19] L. Ackermann, R. Vicente, H. K. Potukuchi, V. Pirovano, *Org. Lett.* **2010**, *12*, 5032 – 5035.

[20] C. Kashima, S. Hibi, T. Maruyama, K. Harada, Y. Omote, *J. Heterocycl. Chem.* **1987**, *24*, 637 – 639.

Manuscript received: May 17, 2020
Accepted manuscript online: July 22, 2020
Version of record online: August 25, 2020

